

# Threshold resummation for $Z$ -boson pair production at NNLO+NNLL

**Pulak Banerjee<sup>1,a,b</sup> Chinmoy Dey,<sup>a</sup> M. C. Kumar <sup>a</sup> and Vaibhav Pandey<sup>a</sup>**

<sup>a</sup>*Department of Physics, Indian Institute of Technology Guwahati, Guwahati-781039, India*

<sup>b</sup>*Istituto Nazionale di Fisica Nucleare, Gruppo collegato di Cosenza, I-87036 Arcavacata di Rende, Cosenza, Italy*

*E-mail:* [pulak.banerjee@lnf.infn.it](mailto:pulak.banerjee@lnf.infn.it), [d.chinmoy@iitg.ac.in](mailto:d.chinmoy@iitg.ac.in),  
[mckumar@iitg.ac.in](mailto:mckumar@iitg.ac.in), [vphiitg@iitg.ac.in](mailto:vphiitg@iitg.ac.in)

**ABSTRACT:** The production of a pair of on-shell  $Z$ -bosons is an important process at the Large Hadron Collider(LHC). Owing to its large production cross section at the LHC, this process is very useful for SM precision studies, electroweak symmetry breaking sector as well as to unravel the possible new physics. In this work, we have performed the threshold resummation of the large logarithms that arise in the partonic threshold limit  $z \rightarrow 1$ , up to Next-to-Next-to-Leading Logarithmic (NNLL) accuracy. The presence of the two-loop contributions in the process dependent resummation coefficient  $g_0$  makes the numerical computation a non-trivial task. After matching the resummed predictions to the Next-to-Next-to-Leading order (NNLO) fixed order results, we present the invariant mass distribution to NNLO+NNLL accuracy in QCD for the current LHC energies. We find that in the high invariant mass region ( $Q = 1$  TeV), while the NNLO corrections are as large as 83% with respect to the leading order, the NNLL contribution enhances the cross section by additional few percent, about 4% for 13.6 TeV LHC. In this invariant mass region, the conventional scale uncertainties in the fixed order results get reduced from 3.4% at NNLO to about 2.6% at NNLO+NNLL, and this reduction is expected to be more for higher  $Q$  values.

**KEYWORDS:** Resummation, perturbative QCD, LHC

---

<sup>1</sup>Most of the work has been carried out at IIT Guwahati.

---

## Contents

<b>1</b>	<b>Introduction</b>	<b>1</b>
<b>2</b>	<b>Theoretical Framework</b>	<b>4</b>
<b>3</b>	<b>Numerical Results</b>	<b>7</b>
<b>4</b>	<b>Summary</b>	<b>13</b>
<b>A</b>	<b>Resummation coefficients</b>	<b>15</b>

---

## 1 Introduction

The production of a pair of massive gauge bosons ( $Z$ ) at the Large Hadron Collider (LHC) is an important process which has been studied very well, both theoretically and experimentally. This process offers very clean signals that can be used to test the prediction of the Standard Model (SM) precisely, thanks to their moderately large production cross sections at the current LHC energies. The process can also be used for testing the SM electroweak symmetry breaking mechanism as well as in the study of fundamental weak interactions among elementary particles. Owing to the large coupling between the Higgs and massive gauge bosons, the process plays an important role in the Higgs sector. One of the important decay modes of Higgs is to a pair of massive gauge bosons, either  $ZZ$  or  $WW$ .

The experimental signature of this process typically involves either four charged leptons, two leptons plus missing energy or two leptons plus two jets or four jet events. Out of these, the decay to four charged leptons provides a very clean signal in the collider experiments, which led to the measurement of these final states both at the ATLAS and CMS experiments for different center of mass energies e.g. 5.02 TeV [1], 7 TeV [2–5], 8 TeV [5–10], 13 TeV [10–15] and 13.6 TeV [16]. Such measurements can be used to probe the trilinear gauge couplings as well as to probe the possible hidden new physics . From the theoretical point of view, a similar study can easily be extended to the production of a pair of new massive gauge bosons.

Owing to the importance of this process, a precise knowledge of this process, specifically the production cross sections as well as various kinematic distributions at the current LHC and future high energetic hadron colliders, is very important. In the perturbative quantum chromodynamics (pQCD), the leading order (LO) predictions for this process have been available for a long time [17–20]. It is well known that the LO predictions are unreliable and are contaminated with large theoretical uncertainties. The next-to-leading order (NLO) calculations in pQCD were obtained for both on shell as well as off

shell  $Z$ -bosons decaying to a pair of leptons. The NLO QCD corrections for this process can be found in Refs. [21–26]. The NLO QCD results, matched with parton shower (NLO+PS) has been studied in Monte Carlo programs such as POWHEG [27, 28] and aMC@NLO [29]. The  $ZZ$  production at the LHC has been analyzed in the context of beyond Standard Model scenarios as well [30]. It is to be noted that at the lowest order in the perturbation theory, this is a quark-antiquark-initiated process similar to the Drell-Yan (DY) production of dileptons. However, the  $Z$ -boson pair production process has more similarities to the diphoton production process, as both involve identical particles in the final state, and both are  $t$  and  $u$  channel processes, whereas DY is an  $s$ -channel process ( $s, t$ , and  $u$  being the Mandelstam variables). For the diphoton production process even at LO, simple kinematic cuts are required to avoid divergences in the forward region, whereas for the case of  $ZZ$  production, the mass of the  $Z$ -boson avoids such divergences, and hence the total production cross section is finite even in absence of any kinematic cuts. However, in the high invariant mass region, or in the region where  $Z$ -boson carries much larger kinetic energy compared to the rest mass energy, both the processes can have similar behavior in the cross sections, the special difference being the isolation algorithm to be used in the case of diphoton production process.

Precision studies entail going beyond NLO. However, for the  $Z$ -boson pair production process, even the NNLO results are challenging for both analytical as well numerical calculations. The full NNLO calculations have been carried out in [31–33] in QCD for the quark annihilation process. It is also worth noting that the NNLO corrections are computed for both the on shell  $Z$ -boson [34, 35] case as well as for off shell  $Z$ -bosons [36, 37] followed by their decay to lepton final states. With the availability of two loop helicity amplitudes [33], the differential distributions for the latter case also became possible. Fiducial cross sections and distributions are also available for the vector boson pair production processes [36, 38]. Additionally, the LO process in the gluon fusion channel,  $gg \rightarrow ZZ$ , also contributes at  $\mathcal{O}(\alpha_s^2)$ . In the low invariant mass region, the gluon fluxes for LHC energies are very large and hence the contribution from this channel near the hadronic threshold region is very crucial and cannot be neglected. Going beyond NNLO for  $Z$ -boson pair production processes is a challenging task. On the other hand, for DY and Higgs production this has been achieved. Recently the full  $N^3LO$  results for DY have become available and can be found in Refs. [39–42] and soft-virtual (SV) [43–45] and next-to-soft-virtual (NSV) [46–48] threshold resummations of DY-type processes are available. The Higgs production through gluon fusion channel  $N^3LO$  results are available in [49–53] and SV [54–57] and NSV [46, 58, 59] threshold resummation results are also available. For Higgs production via bottom quark annihilation, SV [60] and NSV [61] resummation results are also available. Rapidity resummation for DY processes are available for SV [62, 63] and NSV [64–67]. Rapidity distribution for the Higgs production at the threshold to third order in the gluon fusion channel can be found in [68]. For the DY type processes, the threshold results up to third order can be found in [44, 69, 70]. This also enables the evaluation of the resummed parton distribution functions (PDFs), which are important for high precision studies in the large and small  $x$  regions. To see the impact of resummed PDF's on DY and Higgs production; see Refs. [71, 72]. Rapidity resummation for gluon fusion channel Higgs production is

available for SV [73] and NSV [64, 74] cases. Rapidity resummation for Higgs production via bottom quark annihilation is also available at NNLO+NNLL in Ref. [75]. Nevertheless, for the  $Z$ -boson pair in the final state, there has been a tremendous effort to go beyond NNLO. Transverse momentum resummation for vector boson pair production is available up to NNLO+ $N^3LL$  [76, 77]. The parton shower matched with NNLO (NNLO+PS) are recently studied using the MINNLOps [78] method for the  $ZZ$  production. The LO matching with parton shower results are available for the gluon fusion channel as well in Ref. [79]. The NLO corrections to this channel have also become available [80–83]. However, their contribution in the high invariant mass region ( $\geq 2000$  GeV) becomes much smaller than those in the quark annihilation channel. The NLO results matching with parton shower (NLO+PS) results for the gluon fusion channel with massless quarks are also available [84]. Finally, at this precision level, the electroweak corrections cannot be ignored for precision studies and the NLO EW corrections to this process have been computed in Refs. [85–87]. Using SCET formalism, threshold resummation for vector boson pair production is available up to NLO+NNLL [88].

While the threshold resummation for the final state onshell  $Z$ -bosons has been achieved to NLO+NNLL level, it is necessary to go beyond this accuracy. The  $Z$ -boson pair production cross section has been measured at the LHC experiments using 13 TeV data obtained from the  $137\text{ fb}^{-1}$  luminosity. The measured total production cross section is  $17.4\text{ pb}$  with an error of about  $0.8\text{ pb}$  [15]. The invariant mass distribution also has been measured up to 1 TeV region. With the upcoming High-Luminosity LHC (HL-LHC), the integrated luminosity is expected to reach  $3000 - 4000\text{ fb}^{-1}$ , which allows the measurement of  $ZZ$  events in this TeV region with more statistical data. Considering DY production of a lepton pair, the threshold resummation is known till  $N^3LO + N^3LL$  accuracy. In Ref. [44], invariant mass regions around 3 TeV were studied, which is also the same mass range for which experimental results exist in Ref. [89]. The experimental uncertainty reported for the DY process for the invariant mass in the  $Q$  range  $1000 - 1500$  GeV at 7 TeV LHC [90], is around 50%, which decreases by 25% for the 13 TeV in the same  $Q$ -range [89]. From the theory side, for the same  $Q = 1.5$  TeV, the scale uncertainties decrease from 0.77% at NNLO level to about 0.28% at NNLO+NNLL level after incorporating threshold resummation [44].

For the planned FCC-hh [91], the increase in parton fluxes along with the integrated luminosity of  $20 - 30\text{ ab}^{-1}$  can enhance the invariant mass distributions by a few orders of magnitude, thus allowing the measurement of the  $ZZ$  events beyond 1 TeV region even more precisely. At this level of experimental precision, adequate theoretical predictions are necessary. In this work, we attempt to increase the theoretical precision by performing the resummation at NNLL accuracy and give the results after matching them to the available fixed-order results at the NNLO level.

Our paper is organized as follows: we present the theoretical framework in Sec. 2. Details of the phenomenological analysis and the numerical results are presented in Sec. 3. Finally, in Sec. 4, we summarize our observations.

## 2 Theoretical Framework

The hadronic cross section for  $Z$ -boson pair production can be written in terms of its partonic counterpart as follows:

$$\frac{d\sigma}{dQ} = \sum_{a,b=\{q,\bar{q},g\}} \int_0^1 dx_1 \int_0^1 dx_2 f_a(x_1, \mu_F^2) f_b(x_2, \mu_F^2) \int_0^1 dz \delta(\tau - zx_1 x_2) \frac{d\hat{\sigma}_{ab}}{dQ}. \quad (2.1)$$

Here  $Q$  is the invariant mass of the final states. The hadronic and partonic threshold variables  $\tau$  and  $z$  are defined as

$$\tau = \frac{Q^2}{S}, \quad z = \frac{Q^2}{s}, \quad (2.2)$$

where  $S$  and  $s$  are the hadronic and partonic center of mass energies, respectively.  $\tau$  and  $z$  are thus related by  $\tau = x_1 x_2 z$ .

The leading order DY type parton level process has the generic form

$$q(p_1) + \bar{q}(p_2) \rightarrow Z(p_3) + Z(p_4). \quad (2.3)$$

The LO cross-section  $\hat{\sigma}_{q\bar{q}}^{(0)}$  for  $Z$ -boson pair production can be written as,

$$\frac{d\hat{\sigma}_{q\bar{q}}^{(0)}}{dQ} = \frac{1}{2s} \int dPS_2 \mathcal{M}_{(0,0)}, \quad (2.4)$$

where  $dPS_2$  is the two-body phase space integration and  $\mathcal{M}_{(0,0)}$  is the born amplitude, which in  $d = 4 - 2\epsilon$  dimensions is given below,

$$\begin{aligned} \mathcal{M}_{(0,0)} = & B_f N (c_a^4 + 6c_a^2 c_v^2 + c_v^4) \frac{4}{t^2 u^2} \left\{ -m_z^4 t^2 + 8m_z^4 t u + t^3 u - m_z^4 u^2 + t u^3 - 4m_z^2 t u (t + u) \right. \\ & + \epsilon (-2m_z^4 t^2 - 6m_z^4 t u - 2t^3 u + 2m_z^4 u^2 + 2t^2 u^2 - 2t u^3 + 4m_z^2 t u (t + u)) \\ & \left. + \epsilon^2 (-m_z^4 t^2 - 2m_z^4 t u + t^3 u - m_z^4 u^2 + 2t^2 u^2 + t u^3) \right\}. \end{aligned} \quad (2.5)$$

In Eq. (2.5) the kinematical variables  $s, t$ , and  $u$  are defined as

$$(p_1 + p_2)^2 = s, \quad (p_1 - p_3)^2 = t, \quad (p_2 - p_3)^2 = u \quad \text{and} \quad s + t + u = 2m_z^2, \quad (2.6)$$

$$B_f = \frac{(4\pi\alpha)^2}{4N^2}, \quad c_v = \frac{(T_3^f - 2 \sin^2\theta_w Q_f)}{2 \sin\theta_w \cos\theta_w}, \quad c_a = \frac{1}{4 \sin\theta_w \cos\theta_w},$$

where the  $Q_f$  and  $T_3^f$  are the electric charge and the third component of weak isospin of the fermion  $f$  and  $\theta_w$  is the weak mixing angle. Here,  $m_z$  is the mass of the  $Z$ -boson,  $N$  is the  $SU(N)$  color, and  $\alpha$  is the fine structure constant. Here, we have dealt with  $\gamma_5$  in  $d$ -dimension using Larin's prescription [92].

Beyond LO, the partonic cross-section receives corrections originating from virtual and real

contributions. It is interesting to study the cross section in the soft limit, which is defined by,  $z \rightarrow 1$ . This means that the initial partonic center of mass energy is almost used to produce the final state pair of  $Z$ -bosons, and small energy is left to produce soft partons. In this limit, the partonic cross section can be organized as follows:

$$\frac{d\hat{\sigma}_{ab}}{dQ} = \frac{d\hat{\sigma}_{ab}^{(0)}}{dQ} \left( \Delta_{ab}^{\text{sv}}(z, \mu_F^2) + \Delta_{ab}^{\text{reg}}(z, \mu_F^2) \right). \quad (2.7)$$

The term  $\Delta_{ab}^{\text{sv}}$  is known as the soft-virtual (SV) partonic coefficient and captures all the singular terms in the  $z \rightarrow 1$  limit. Only quark-antiquark or gluon-gluon subprocesses contribute to this SV cross section. The  $\Delta_{ab}^{\text{reg}}$  term contains regular (hard) contributions in the variable  $z$ . Both these contributions are expanded in a perturbative series of the strong coupling constant. In our work, we consider such an expansion up to NNLO in QCD. It is to be noted that the overall normalization factor  $d\hat{\sigma}_{ab}^{(0)}/dQ$  depends on the process under study.

The singular part of the partonic coefficient has a universal structure which gets contributions from the underlying hard form factor [49, 93–96], mass factorization kernels [97–99] and soft radiations [100–114]. According to the KLN theorem, these infrared divergences, when regularized and combined, yield finite contributions. After the infrared cancellation, the finite part of these has the universal structure in terms of  $\delta(1 - z)$  and plus distributions  $\mathcal{D}_i = [\ln(1 - z)^i/(1 - z)]_+$ . In the threshold limit,  $z \rightarrow 1$ , the plus distributions contribute dominantly to the SV cross section. These large distributions can be resummed to all orders in the threshold limit. Threshold resummation is conveniently performed in the Mellin ( $N$ ) space where the convolution structures become simple product.

The partonic coefficient in the Mellin space is organized as follows:

$$\hat{\sigma}_N^{\text{NNLL}} = \int_0^1 dz z^{N-1} \Delta_{ab}^{\text{sv}}(z) \equiv g_0 \exp(G_N). \quad (2.8)$$

The factor  $g_0$  is independent of the Mellin variable, whereas the threshold enhanced large logarithms ( $\ln^i N$  in Mellin space) are resummed through the exponent  $G_N$ . The resummed accuracy is determined through the successive terms from the exponent  $G_N$  which up to NNLL takes the form,

$$G_N = \ln(\bar{N}) \bar{g}_1(\bar{N}) + \bar{g}_2(\bar{N}) + a_s \bar{g}_3(\bar{N}) + \dots \quad (2.9)$$

where  $\bar{N} = N \exp(\gamma_E)$ . These coefficients are universal and only depend on the partonic flavors being either quark or gluon. Their explicit form can be found in Refs. [111, 115]. In order to achieve complete resummed accuracy one also needs to know the  $N$ -independent coefficient  $g_0$  up to sufficient accuracies. In particular, up to NNLL, it takes the form,

$$g_0 = 1 + a_s g_{01} + a_s^2 g_{02} + \dots \quad (2.10)$$

where  $a_s = \frac{\alpha_s}{4\pi}$  and  $\alpha_s$  is the strong coupling constant. Using the universal  $G_N$  and the process dependent  $g_0$ , resummation for two Higgs boson production in the gluon fusion channel at  $\text{N}^3\text{LO} + \text{N}^3\text{LL}$  has been achieved in [116].

It is also possible to resum part (or all) of the  $g_0$  by including them in the exponent [54, 55, 117–119], which, however, have a subleading effect as these contributions are not dominated in the threshold region.

The  $N$ -independent coefficient  $g_0$  is computed based on the formalism given in Ref. [120], the expression for  $g_{01}$  and  $g_{02}$  are given in Appendix A. The  $g_{01}$  requires one-loop virtual computations ( $\mathcal{M}_{(0,1)}$ ); we have computed the amplitude  $\mathcal{M}_{(0,1)}$  using our inhouse **FORM** [121] code and the expression is given in Appendix A. To obtain the results in  $z$  space, one needs to do the Mellin inversion as,

$$\frac{d\sigma^{\text{N^nLL}}}{dQ} = \frac{d\hat{\sigma}^{(0)}}{dQ} \sum_{a,b \in \{q,\bar{q}\}} \int_{c-i\infty}^{c+i\infty} \frac{dN}{2\pi i} \tau^{-N} f_{a,N}(\mu_F) f_{b,N}(\mu_F) \hat{\sigma}_N^{\text{N^nLL}}. \quad (2.11)$$

This complex integral contains the Landau pole at  $N = \exp(1/(2a_s\beta_0) - \gamma_E)$ , which makes the choice of contour very important. The Mellin inversion is performed [122] along the contour  $N = c + x \exp(i\phi)$ , where  $x$  is real variable. Following the *minimal prescription* [123], we choose the value of  $c$  such that all the singularities except the Landau pole lie on the left side of the integration contour. For numerical results we choose  $c = 1.9$  and  $\phi = 3\pi/4$ . It may be noted that the results are dependent on the choice of the prescription. Several studies have been done in the past in this direction [124–128]. It is to be noted that there are other prescriptions to deal with the Landau pole like Borel prescription [55]. Although these prescriptions differ by subleading terms, they give similar numerical results in the high  $Q$  region [55].

Finally, the matched results can be written as,

$$\begin{aligned} \frac{d\sigma^{\text{N^nLO+N^nLL}}}{dQ} = & \frac{d\sigma^{\text{N^nLO}}}{dQ} + \frac{d\hat{\sigma}^{(0)}}{dQ} \sum_{a,b \in \{q,\bar{q}\}} \int_{c-i\infty}^{c+i\infty} \frac{dN}{2\pi i} \tau^{-N} f_{a,N}(\mu_F) f_{b,N}(\mu_F) \\ & \times \left( \hat{\sigma}_N^{\text{N^nLL}} - \hat{\sigma}_N^{\text{N^nLL}} \Big|_{\text{tr}} \right). \end{aligned} \quad (2.12)$$

In the above equation,  $f_{a,N}$  in the Mellin transformed PDF, which one can obtain using publicly available code such as QCD-PEGASUS [122]. However, for numerical applications, it can also be approximated by employing the  $z$ -space PDF following Refs. [105, 115]. The last term in the bracket of Eq. (2.12) indicates the truncation of the resummed partonic coefficient Eq. (2.8), which avoids double counting the regular terms already present in the fixed order.

Before we proceed to the numerical results, we add a few comments on the extraction of the resummation coefficient,  $g_{02}$ , which is a process-dependent quantity. To obtain the full  $g_{02}$ , we follow the procedure given in Ref. [120] and make use of the two-loop ( $\mathcal{M}_{(0,2)}$ ) amplitudes as well as the one-loop squared amplitudes, ( $\mathcal{M}_{(1,1)}$ ). The two-loop virtual amplitudes  $\mathcal{M}_{(0,2)}$  are reconstructed using the **WWamp** package [33], while the  $\mathcal{M}_{(1,1)}$  is obtained by squaring  $\mathcal{M}_{(0,1)}$ . After performing the UV renormalization, the IR pole structure of these amplitudes is then verified using Catani's I-operator formalism [129]. The finite parts of the two-loop amplitudes are quite large in size. These amplitudes are then simplified and optimized using our inhouse-developed **FORM** routines. We have

used `handyG` [130] for numerical evaluations of the generalized polylogarithms in these one-loop and two-loop amplitudes. Finally, these two-loop amplitudes have been cross-checked numerically for different phase space points with those implemented in the `MATRIX` [33, 131–135]. The resummation formalism used here is developed in [62, 73, 105] and has been successfully used in the past in calculating NNLO+NNLL and  $N^3LO+N^3LL$  for Drell-Yan processes [43, 44, 56, 136]. All the anomalous dimensions required for computing the resummed results are given in the Appendix A.

### 3 Numerical Results

In this section, we present the numerical results for the  $Z$ -boson pair production process at the LHC. For the numerical computation, we take the fine structure constant to be  $\alpha = 1/132.233193$ . The mass of the weak gauge bosons  $m_z = 91.1876$  GeV,  $m_w = 80.385$  GeV. The Weinberg angle is  $\sin^2\theta_w = (1 - m_w^2/m_z^2) = 0.222897223$ . This corresponds to the weak coupling  $G_F = 1.166379 \times 10^{-5}$  GeV $^{-2}$ . The default choice of centre mass energy of the incoming protons is 13.6 TeV. Unless specified otherwise, in our numerical analysis, we use MSHT20 [137] parton distribution functions (PDFs) throughout, taken from the LHAPDF [138]. The LO, NLO and NNLO cross sections are obtained by convoluting the respective coefficient functions with MSHT20lo\_as130, MSHT20nlo\_as120 and MSHT20nnlo\_as118 PDF sets, using the central set (iset=0) as the default choice. The strong coupling constant  $a_s$  is taken from LHAPDF [138], and it varies order by order in the perturbation theory. For our analysis, we consider the number of light quark flavors as  $n_f = 5$ . For the fixed-order calculations, we have used the package `MATRIX` [131]. The fixed-order results from `MATRIX` are checked against those obtained from the `MadGraph` package [139] up to NLO and are found to be in good agreement. The fixed-order NNLO results have been checked with the numbers quoted in the literature [34, 36]. The resummation results are obtained using the inhouse developed numerical code. The unphysical renormalization and factorization scales are set to  $\mu_R = \mu_F = Q$ , where  $Q$  is the invariant mass of the  $Z$ -boson pair production in the final state. The scale uncertainties are estimated by varying the unphysical scales in the range so that  $|\ln(\mu_R/\mu_F)| \leq \ln 2$ . The symmetric scale uncertainty is calculated from the maximum of the absolute deviation of the cross section from that obtained with the central/default scale choice.

We first comment on how much the SV results are in comparison to the full fixed-order cross section. The SV results contain distributions, which contribute significantly in the threshold region. We find that at the SV corrections at the one-loop level are about about 79% of the full first order correction at  $Q=595$  GeV, and this contribution increases to 94% at  $Q= 995$  GeV. Similarly, at NNLO level, the second-order SV contributions contribute about 57% of the full second-order result at  $Q=595$  GeV, and this contribution increased to 80% at  $Q = 995$  GeV. A similar observation of large SV contributions has been reported in [68] in the context of Drell-Yan production of di-leptons. With the available ingredients i.e. (without the three loop virtual corrections) it is also possible to estimate the size of the soft-gluon contributions at three loop level. The SV corrections thus computed at three loop level are found to be around 0.2% of LO.

To estimate the impact of the higher-order corrections from FO and resummation, we define the following ratios of the cross sections which are useful in the experimental analysis:

$$K_{ij} = \frac{\sigma_{N^i LO}}{\sigma_{N^j LO}}, \quad R_{ij} = \frac{\sigma_{N^i LO + N^i LL}}{\sigma_{N^j LO}} \quad \text{and} \quad L_{ij} = \frac{\sigma_{N^i LO + N^i LL}}{\sigma_{N^j LO + N^j LL}} \quad \text{with } i, j = 0, 1 \text{ and } 2. \quad (3.1)$$

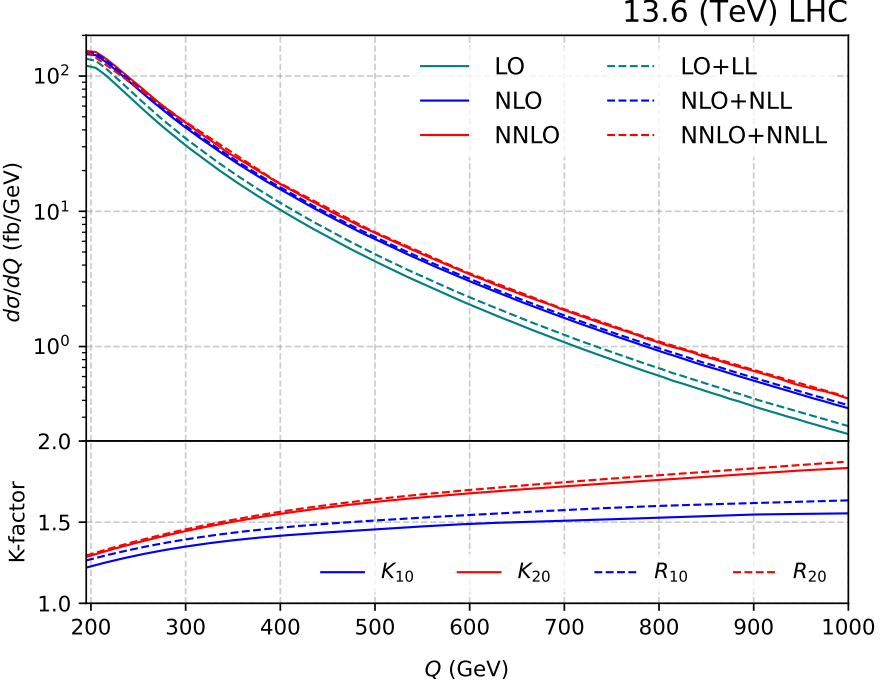


**Figure 1.** Resummed predictions for the  $Z$ -boson pair invariant mass distribution (upper panel) and the corresponding K-factors(lower panel) up to NNLO+NNLL.

In Fig. [1] , we present the fixed-order results for the invariant mass distribution of the  $Z$ -boson pair production from  $2m_z$  to 1300 GeV up to NNLO+NNLL in QCD. For the range of  $Q$ -variation considered here, the distribution varies over three orders of magnitude. In the lower panel, the corresponding fixed-order as well as the resummed K-factors, as defined in Eq. (3.1) are given. The NLO K-factor  $K_{10}$  here varies from about 1.22 at  $Q = 200$  GeV to about 1.58 at  $Q = 1300$  GeV. As can be seen from Fig. [1], the variation of  $K_{10}$  above  $Q = 500$  GeV is mild. However, the NNLO K-factor  $K_{20}$  slowly but continuously increases from about 1.29 to about 1.94 for the  $Q$  range considered here. This clearly shows additional contributions coming from second-order corrections in the higher  $Q$ -region, which are due to the real correction subprocesses like  $qq' \rightarrow ZZqq'$ . A more detailed discussion of this kind of contributions can be found in the Ref. [86]. The resummation has been achieved in the Mellin space where large logarithms of kind  $\ln(\bar{N})$  have been resummed to NNLL accuracy as outlined in the text. From  $R_{00}$ , we see that the LL resummation enhances the LO results by about 15% for  $Q = 1300$  GeV. While the NLO corrections are as big as 58%,

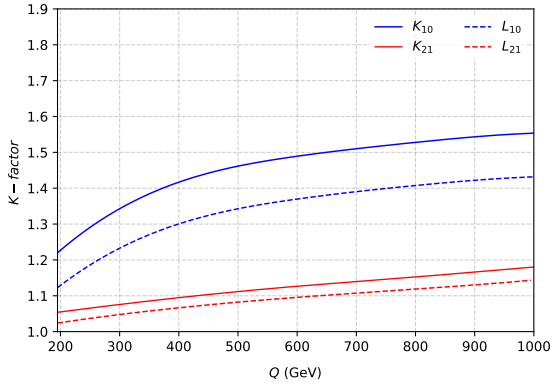


**Figure 2.** K-factors for the fixed-order and resummed results for  $Z$ -boson pair production (see Eq. (3.1) for details).

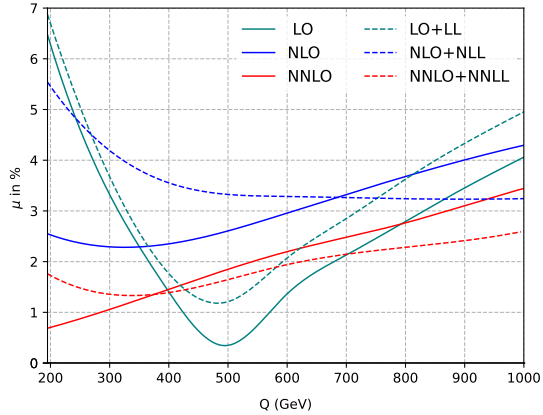


**Figure 3.** Seven point scale uncertainties for  $Z$ -boson pair production up to NNLO+NNLL.

the corresponding NLO+NLL results are about 68% of LO for the same  $Q$  region. The corresponding contribution from NNLO is about 94% where the NNLL resummation adds an additional few percent, making the NNLO+NNLL contributions sizable, about 99% of LO.

To better estimate the size of higher-order corrections beyond a certain fixed-order as well as that of resummed contributions at different logarithmic accuracy, we present various K-factors of the kind  $K_{i,i-1}$ ,  $R_{i,i-1}$  and  $L_{i,i-1}$ , in Fig. [2]. We notice that, in general,  $L_{ij}$  are smaller compared to the respective  $K_{ij}$ , indicating that the threshold logarithms of a given accuracy (LL, NLL, ...) capture a substantial contribution of the higher-order corrections. Moreover, we notice that the gap between  $K_{21}$  and  $L_{21}$  is smaller than that between  $K_{10}$  and  $L_{10}$ , demonstrating a nice convergence of the higher-order QCD corrections. Further, it is evident that the former gap is almost independent of  $Q$  while the latter gap increases with  $Q$ . We also notice that while the  $L_{10}$  is about as large as 1.45, the  $L_{21}$  is smaller and is about 1.18. This indicates that the contribution of the second-order terms and the tower

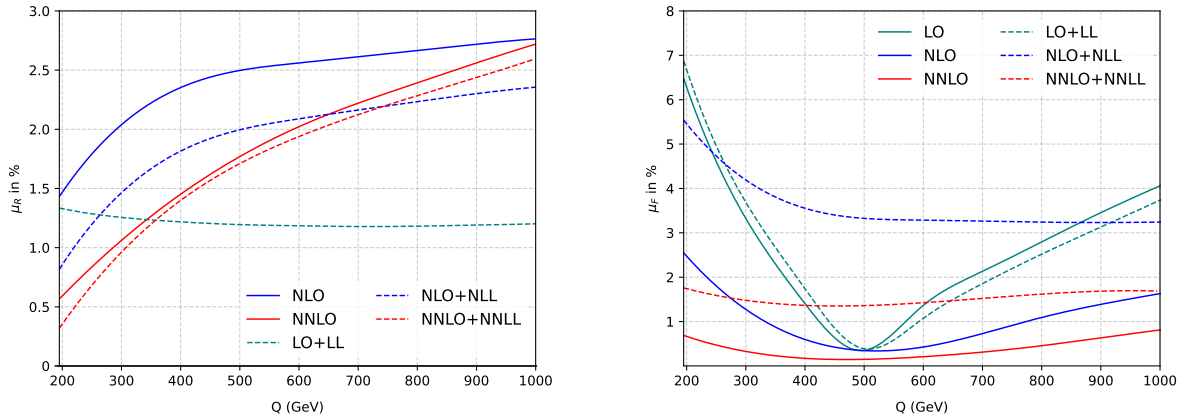


**Figure 4.** Renormalization(left) and factorization(right) scale uncertainties for  $Z$ -boson pair production up to NNLO+NNLL.

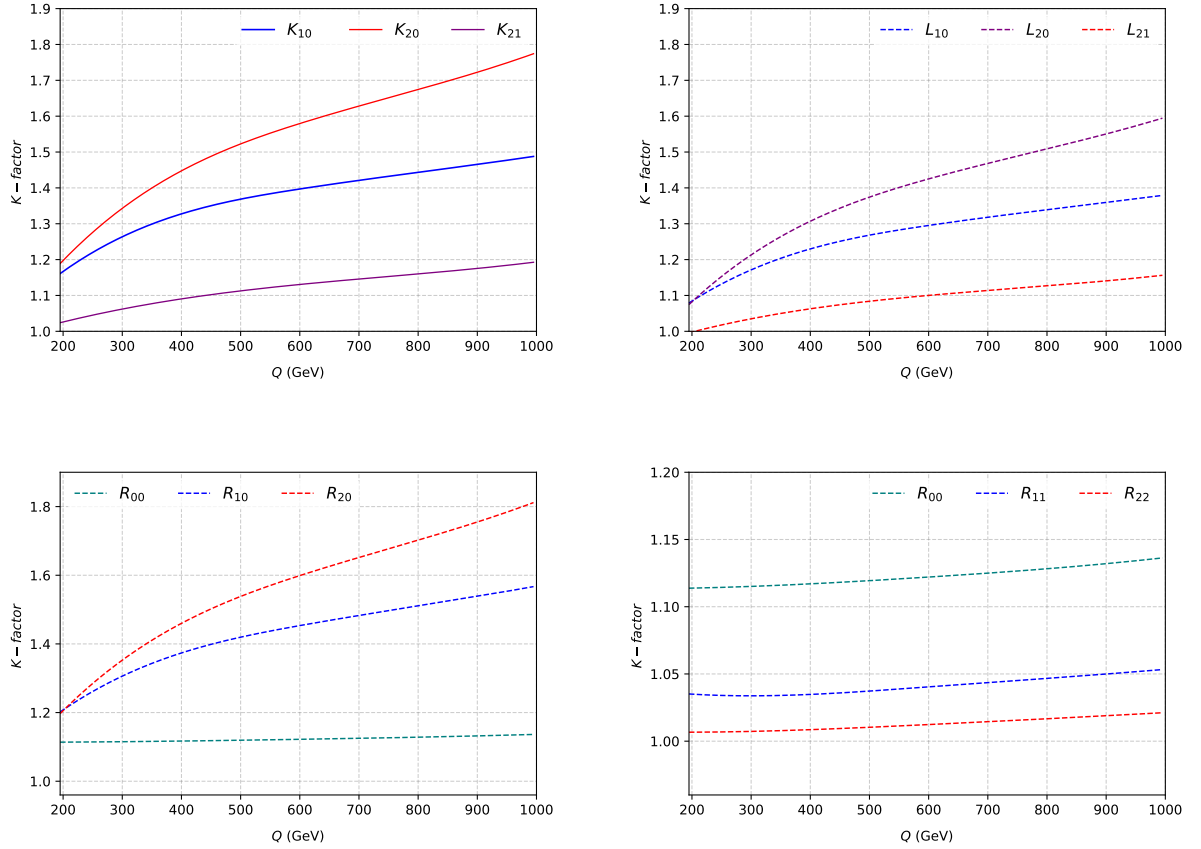


**Figure 5.** K-factors as defined in Eq. (3.1) but using same NNLO PDFs at various orders in the perturbation theory.

of further sub-leading logarithms (NNLL) that are not included in NLO+NLL are about

18% of NLO+NLL, and are still non-negligible for precision studies.

The underlying theory uncertainties in these distributions up to NNLO+NNLL due to the variation of arbitrary factorization and renormalization scales are presented in Fig. [3]. Here, the complete 7-point scale variations, as discussed in the text, have been presented where the maximum uncertainty in the low  $Q$ -region at LO is about 6.5%. However, the inclusion of higher-order NLO and NNLO corrections reduce this uncertainty to as low as 2.6% and to less than 1.0% respectively, for  $Q = 200$  GeV. The general observation is that these scale uncertainties are found to increase with  $Q$ , which for the NNLO case are found to change from about 0.7% to about 4.5%.

For higher  $Q$  values, the threshold logarithms are dominant and as a result of resummation, the corresponding scale uncertainties are expected to be smaller than those in the fixed-order ones. We see that the scale uncertainties increase from LO to LO+LL, this is because for the process under study there is no  $\mu_R$  scale dependence at LO. On the other hand, the 7-point scale uncertainties at NLO+NLL (NNLO+NNLL) become smaller than those at NLO(NNLO) beyond  $Q = 700(400)$  GeV. While for NNLO, the scale uncertainties reach up to 4.5% in high  $Q$  regions, the corresponding ones at NNLO+NNLL level reach up to 3.2%.

In the low  $Q$  region, the resummation is found to enhance the scale uncertainties compared to the corresponding fixed-order results. This is due to the fact that in the low  $Q$  region, the regular terms coming from the hard non-collinear gluons as well as those from the other parton channels are also important. However being nonuniversal, they cannot be resummed to all orders in the perturbation theory. As a result, the resummation cannot improve the scale uncertainties in the fixed-order results in the low  $Q$  region.

In the left panel of Fig. [4], we present the uncertainties due to only the renormalization scale by keeping the  $\mu_F = Q$  fixed. Similarly, in the right panel, the uncertainties due to only factorization scale variations for fixed  $\mu_R = Q$  are given. It is also worth noting that while performing the resummation, the large partonic threshold logarithms are resummed to all orders in the perturbation series that is expanded in  $a_s$ , and hence the uncertainties due to  $\mu_R$  are expected to be smaller for a given  $\mu_F$  as shown in the left panel of Fig. [4]. However, the scale  $\mu_F$  enters both the PDFs as well as the parton coefficient functions. The uncertainty due to  $\mu_F$  need not decrease as a result of resummation where the PDFs used are extracted at a particular fixed-order. Such a behavior of  $\mu_F$  scale uncertainty can be seen in the right panel of Fig. [4] and has already been reported in the literature [43–47, 58–60, 62, 73, 74, 140, 141].

To study the convergence of the perturbation series, it is useful to keep the PDFs fixed and study how the cross sections vary at different orders. For this, we present the K-factors obtained from the invariant mass distribution computed with NNLO PDFs, to NNLO+NNLL accuracy. Thus, the same  $a_s$  is used both at NLO and NNLO. In the top left panel of Fig. [5], we present the fixed-order K-factors,  $K_{10}$ ,  $K_{20}$  and  $K_{21}$ . For a faster converging perturbation series, the factor  $K_{i,i-1}$  is supposed to be as close to unity as possible. While the  $K_{10}$  has the usual NLO K-factor information and is as large as 55%, from the  $K_{21}$  we see that the NNLO corrections could contribute an additional 25% of NLO results. From the behavior of  $K_{21}$ , we see that the second-order corrections are small, but

they increase with  $Q$ . Similar results are presented but for  $L_{ij}$  in the top right panel of Fig. [5]. By definition, these ratios will estimate the contribution of higher-order corrections over and above at least LO+LL level. Hence, these are smaller than the corresponding fixed-order K-factors  $K_{ij}$ . In the bottom left panel of Fig. [5], we present the resummed K-factors  $R_{i0}$  to estimate the size of the resummed results above the LO predictions. We notice that the difference  $(R_{20} - R_{10})$  is less than  $(R_{10} - R_{00})$  for the whole invariant mass region considered here. In the bottom right panel of Fig. [5], we plot  $R_{ii}$  that gives the information about the resummed contributions over and above the corresponding fixed-order corrections. We notice that the contribution from the resummed corrections for any given  $i$  is smooth but slowly increasing as  $Q$  increases. From  $R_{22}$ , we can estimate the size of higher logarithmic terms beyond NNLO to be around 2.8% of NNLO for  $Q = 1300$  GeV.

The total production cross sections, after integrating over the invariant mass region over the full kinematic region, for LHC energies are substantially large for the  $Z$ -boson pair production process. These production cross sections have been given in the Tab. [1] up to NNLO+NNLL accuracy, along with the theory uncertainties due to the seven-point scale variations for different centre of mass energies of the incoming protons. We notice that for any given centre of mass energy, the cross sections increase while the uncertainties decrease as we go from LO to NLO, in the fixed-order case. However, the uncertainties will increase from NLO to NNLO due to the gluon fusion channel opening up from the second-order in perturbation theory, and hence new contributions will add up to the renormalization scale uncertainties. The gluon fluxes for the LHC energies near the  $2m_z$  region are quite large, and this gluon fusion channel contributes about 9.3% of LO  $Z$ -boson pair production at 13.6 TeV LHC energy. To systematically quantify the uncertainties in the perturbation theory, we define the second-order cross section without this gluon fusion channel and call it NNLO $_{q\bar{q}}$ . The scale uncertainties in the total production cross sections, LO, NLO and NNLO $_{q\bar{q}}$  are found to systematically decrease from 4.24% to 1.07% for 13.6 TeV LHC energy. This behavior remains similar for other centre of mass energies. We notice a similar behavior in the total production cross sections after the resummation has been performed, i.e. the scale uncertainties decrease from 4.62% to 1.42%, as we go from LO+LL to NNLO+NNLL. However, the NNLO $_{q\bar{q}}$ +NNLL has a somewhat larger scale uncertainty compared to the one in NNLO $_{q\bar{q}}$ . This is simply because of the definition of total production cross section where the invariant mass has been integrated out from  $Q_{\min} = 2m_z$  to  $\sqrt{S}$ . In the lower  $Q$ -region the contribution from other channels like  $qg$ -subprocess cannot be ignored. However, with increasing  $Q_{\min}$  in the total production cross section, the scale uncertainties in NNLO $_{q\bar{q}}$ +NNLL are expected to be smaller than those in NNLO $_{q\bar{q}}$ , as evident from Fig. [3]. The NLO corrections for the gluon fusion channel, in the massless quark limit, are about 68% of its LO for the current LHC energies [80]. The inclusion of massive top quark loops is found to increase this correction to about 73% [83]. Finally, at this NNLO+NNLL accuracy in the perturbation theory, the NLO EW correction for  $Z$ -boson pair production also becomes important. The EW corrections are negative, and for total production, they are found to be around  $-6.2\%$ , while the mixed NNLO QCD $\times$ EW corrections are about  $-5.7\%$  for 13 TeV LHC. For the invariant mass distribution, the EW corrections amount to  $-15\%$  at 1 TeV [86]. Finally, the NNLO+NNLL results match well

within the theoretical and experimental uncertainties to the ATLAS [12] and CMS [13] measurements of the  $Z$ -boson pair production cross section at 13 TeV. The NNLO+NNLL enhances the NNLO cross section by 0.6% of NNLO at 13 TeV. We also note that the uncertainties due to the non-perturbative PDFs are also important. These PDF uncertainties for the  $q\bar{q}$  initiated DY processes are found to be about 3% around the 1 TeV region [44]. The  $ZZ$  production process also takes place via  $q\bar{q}$  initial states, and hence a similar PDF uncertainty is expected around  $Q = 1$  TeV.

$\sqrt{S}$	13.0 TeV	13.6 TeV	100.0 TeV
LO	$10.958 \pm 4.00\%$ pb	$11.664 \pm 4.24\%$ pb	$138.617 \pm 13.84\%$ pb
NLO	$14.380 \pm 1.92\%$ pb	$15.284 \pm 1.91\%$ pb	$169.090 \pm 5.13\%$ pb
NNLO <sub><math>q\bar{q}</math></sub>	$15.427 \pm 1.01\%$ pb	$16.437 \pm 1.07\%$ pb	$184.438 \pm 1.69\%$ pb
NNLO	$16.418 \pm 2.22\%$ pb	$17.521 \pm 2.30\%$ pb	$212.344 \pm 3.81\%$ pb
LO+LL	$12.353 \pm 4.37\%$ pb	$13.143 \pm 4.62\%$ pb	$153.653 \pm 14.10\%$ pb
NLO+NLL	$14.890 \pm 4.49\%$ pb	$15.824 \pm 4.56\%$ pb	$174.162 \pm 7.76\%$ pb
NNLO <sub><math>q\bar{q}</math></sub> +NNLL	$15.527 \pm 1.39\%$ pb	$16.543 \pm 1.42\%$ pb	$185.348 \pm 2.53\%$ pb
NNLO+NNLL	$16.518 \pm 1.84\%$ pb	$17.627 \pm 1.93\%$ pb	$213.254 \pm 3.64\%$ pb
ATLAS (13.0 TeV) [12]	$17.3 \pm 0.9$ pb		
CMS (13.0 TeV) [13]	$17.2 \pm 1.0$ pb		

**Table 1.** Inclusive cross section for  $Z$ -boson pair production for different center of mass energies of the incoming protons, along with the corresponding 7-point scale uncertainties. Also, the ATLAS [12] and CMS[13] measurements with the total uncertainty from statistical, systematic and luminosity uncertainties involved in the measurement.

## 4 Summary

To summarize, we have performed the threshold resummation for the production of a pair of  $Z$ -bosons at the energies of LHC, by resumming the threshold logarithms to NNLL accuracy in QCD. The final state having two massive particles makes the process dependent one-loop and two-loop virtual corrections more difficult compared to the massless final state like di-lepton or di-photon, or one-massive final state like Higgs boson. The presence of such virtual amplitudes makes the resummation a challenging task to achieve numerically, in contrast to the case of  $2 \rightarrow 1$  processes like DY and Higgs production cross-section processes. It is also worth noting that compared to the previously available NLO+NNLL results, in the present NNLO+NNLL results, the presence of real corrections is also equally important and thanks to MATRIX where such contributions have already been taken into account. In this work, we have performed this resummation by systematically matching to the known fixed order NNLO results (from the package MATRIX) and present our phenomenological results to NNLO+NNLL accuracy for both the total production cross sections as well as for the invariant mass distribution of the  $Z$ -boson pair, for the current LHC energies, 13.0 and 13.6 TeV, as well as for the upcoming future 100 TeV collider. We notice that the NNLL resummed results in general enhance the cross sections and contribute an additional few

percent to the known NNLO results. After performing the resummation at NNLO+NNLL accuracy, our results for the total production at 13 TeV center of mass energy are found to agree with experimental measurements (within the reported errors) from the ATLAS and CMS. We have also presented the theory uncertainties by varying the unphysical renormalization and factorization scales from  $Q/2$  to  $2Q$ . We find that, after performing the resummation, the scale uncertainties of about 4.5% in NNLO cross sections get reduced to about 3.2% at NNLO+NNLL level for the invariant mass region  $Q = 1.3$  TeV.

The availability of these resummed results is expected to provide a foundation for future theoretical and experimental studies of diboson processes at the LHC and beyond.

### Acknowledgements

The research work of M.C.K. is supported by SERB Core Research Grant (CRG) under the project CRG/2021/005270. The work of P.B. is supported by the INFN/QFT@COLLIDERS project (Italy). The authors would like to thank A. H. Ajjath, M. Bonvini, L. Buonocore, G. Das and V. Ravindran for useful discussions. We acknowledge National Supercomputing Mission (NSM) for providing computing resources of ‘PARAM Kamrupa’ at IIT Guwahati, which is implemented by C-DAC and supported by the Ministry of Electronics and Information Technology (MeitY) and Department of Science and Technology (DST), Government of India, where most of the computational work has been carried out.

## A Resummation coefficients

The process-dependent  $g_0$  coefficients defined in Eq. (2.10) are given as (defining  $L_{qr} = \ln(Q^2/\mu_R^2)$ ,  $L_{fr} = \ln(\mu_F^2/\mu_R^2)$ ),

$$g_{01} = 2\mathcal{K}_{(0,1)} + 2C_F \left\{ -3L_{fr} + L_{qr}^2 + \zeta_2 \right\}, \quad (\text{A.1})$$

$$\begin{aligned} g_{02} = & \mathcal{K}_{(1,1)} + 2\mathcal{K}_{(0,2)} + C_F n_f \left\{ -\frac{328}{21} + \frac{2}{3}L_{fr} + \frac{112}{27}L_{qr} - \frac{20}{9}L_{qr}^2 - \frac{10}{9}\zeta_2 + \frac{16}{3}L_{fr}\zeta_2 \right. \\ & - \frac{4}{3}L_{qr}\zeta_2 + \frac{32}{3}\zeta_3 \left. \right\} + C_F^2 \left\{ -3L_{fr} + 18L_{fr}^2 - 12L_{fr}L_{qr}^2 + 2L_{qr}^4 + 12L_{fr}\zeta_2 + 4L_{qr}^2\zeta_2 \right. \\ & + 2\zeta_2^2 - 48L_{fr}\zeta_3 \left. \right\} + C_F \left\{ +3\beta_0 L_{fr}^2 - \frac{2}{3}\beta_0 L_{qr}^3 - 12L_{fr}\mathcal{K}_{(0,1)} + 4L_{qr}^2\mathcal{K}_{(0,1)} \right. \\ & - 2\beta_0 L_{qr}\zeta_2 + 4\mathcal{K}_{(0,1)}\zeta_2 + \frac{46}{3}\beta_0\zeta_3 \left. \right\} + C_F C_A \left\{ +\frac{2428}{81} - \frac{17}{3}L_{fr} - \frac{808}{27}L_{qr} + \frac{134}{9}L_{qr}^2 \right. \\ & + \frac{67}{9}\zeta_2 - \frac{88}{3}L_{fr}\zeta_2 + \frac{22}{3}L_{qr}\zeta_2 - 4L_{qr}^2\zeta_2 - 12\zeta_2^2 - \frac{176}{3}\zeta_3 + 24L_{fr}\zeta_3 + 28L_{qr}\zeta_3 \left. \right\} \quad (\text{A.2}) \end{aligned}$$

Here, we define

$$\mathcal{K}_{(m,n)} = \frac{\mathcal{M}_{(m,n)}^{\text{fin}}}{\mathcal{M}_{(0,0)}} \quad (\text{A.3})$$

where,

$$\mathcal{M}_{(m,n)}^{\text{fin}} \equiv \langle \mathcal{M}_m | \mathcal{M}_n \rangle \quad (\text{A.4})$$

and  $|\mathcal{M}_n\rangle$  represents the UV-renormalized, IR-finite virtual amplitude at the  $n$ -th order in  $a_s$ , as given in Eq. (C3) of Ref. [120]. The one loop virtual contribution for  $Z$ -boson pair production is,

$$\mathcal{M}_{(0,1)} = a_s(\mu_R^2) \frac{\Gamma(1-\epsilon)}{\Gamma(1-2\epsilon)} (4\pi)^\epsilon \left( \frac{\mu_R^2}{s} \right)^\epsilon C_F \left[ -4 \left\{ \frac{1}{\epsilon^2} + \frac{3}{2\epsilon} \right\} \mathcal{M}_{(0,0)} + \mathcal{M}_{(0,1)}^f \right]. \quad (\text{A.5})$$

here,

$$\begin{aligned} \mathcal{M}_{(0,1)}^f = & B_f N(c_v^4 + 6c_v^2c_a^2 + c_a^4) \left( \frac{4}{t^2u^2} \right) \left[ 2\zeta_2 \left( -20m_z^2tu(t+u) - 4m_z^4(t^2 - 8tu + u^2) \right. \right. \\ & + tu(5t^2 + 4tu + 5u^2) + \frac{tu}{\kappa s(4m_z^2 - s)^2} \left( -32m_z^6tu - 64m_z^8(t+u) \right. \\ & + 8m_z^2tu(t+u)^2 - (t+u)^3(3t^2 + 4tu + 3u^2) \\ & \left. \left. + m_z^4(22t^3 + 82t^2u + 82tu^2 + 22u^3) \right) \right) + \ln \left( \frac{s}{m_z^2} \right) \frac{1}{(4m_z^2 - s)^2} \left( \right. \\ & \left. 8m_z^2t^2u^2(t+u) + 12m_z^8(t^2 - 8tu + u^2) - tu(t+u)^2(3t^2 + 4tu + 3u^2) \right) \end{aligned}$$

$$\begin{aligned}
& + 4m_z^6(3t^3 - 5t^2u - 5tu^2 + 3u^3) + m_z^4(3t^4 + 14t^3u + 78t^2u^2 + 14tu^3 + 3u^4) \\
& + \frac{tu}{\kappa s(4m_z^2 - s)^2} (\ln(x) + 4\text{Li}_2(-x)) (-32m_z^6tu - 64m_z^8(t + u) \\
& + 8m_z^2tu(t + u)^2 - (t + u)^3(3t^2 + 4tu + 3u^2) \\
& + m_z^4(22t^3 + 82t^2u + 82tu^2 + 22u^3)) + \frac{1}{(t - m_z^2)(u - m_z^2)(4m_z^2 - s)} ( \\
& 18m_z^{10}(t^2 - 8tu + u^2) + m_z^8(-9t^3 + 131t^2u + 131tu^2 - 9u^3) \\
& - 7t^2u^2(t^3 + t^2u + tu^2 + u^3) - 4m_z^4tu(4t^3 + 23t^2u + 23tu^2 + 4u^3) \\
& + m_z^6(-9t^4 + 14t^3u - 66t^2u^2) + 14tu^3 - 9u^4) \\
& + m_z^2tu(9t^4 + 32t^3u + 82t^2u^2 + 32tu^3 + 9u^4) + \ln\left(\frac{-t}{m_z^2}\right) \frac{u}{(t - m_z^2)^2} ( \\
& 3m_z^8(-4t + u) + 6m_z^6t(2t + u) - 2m_z^2t^2u(4t + u) + 3t^3u(2t + 3u) \\
& + m_z^4t(-2t^2 + tu - 3u^2)) + \left(2\ln\left(\frac{-t}{m_z^2}\right) \ln\left(\frac{t - m_z^2}{m_z^2 s}\right) + 4\text{Li}_2\left(\frac{t}{m_z^2}\right) \right. \\
& \left. - \ln^2\left(\frac{-t}{m_z^2}\right)\right) u(m_z^4(8t - 2u) - 4m_z^2t(2t + u) + t(2t^2 + 2tu + u^2)) \\
& + \ln\left(\frac{-u}{m_z^2}\right) \frac{t}{(u - m_z^2)^2} (3m_z^8(-4u + t) + 6m_z^6u(2u + t) - 2m_z^2u^2t(4u + t) \\
& + 3u^3t(2u + 3t) + m_z^4u(-2u^2 + tu - 3t^2)) + \left(2\ln\left(\frac{-u}{m_z^2}\right) \ln\left(\frac{u - m_z^2}{m_z^2 s}\right) \right. \\
& \left. + 4\text{Li}_2\left(\frac{u}{m_z^2}\right) - \ln^2\left(\frac{-u}{m_z^2}\right)\right) t(m_z^4(8u - 2t) - 4m_z^2u(2u + t) \\
& \left. + u(2u^2 + 2tu + t^2))\right].
\end{aligned}$$

$$x = \frac{1 - \kappa}{1 + \kappa}; \quad \kappa = \sqrt{1 - 4\frac{m_z^2}{s}} \quad (\text{A.6})$$

The process-independent universal resum exponent defined in Eq. (2.9) which are used for DY-type processes are given as,

$$g_1 = \left[ \frac{A_1}{\beta_0} \left\{ 2 - 2 \ln(1 - \omega) + 2 \ln(1 - \omega) \omega^{-1} \right\} \right], \quad (\text{A.7})$$

$$\begin{aligned}
g_2 = & \left[ \frac{D_1}{\beta_0} \left\{ \frac{1}{2} \ln(1 - \omega) \right\} + \frac{A_2}{\beta_0^2} \left\{ -\ln(1 - \omega) - \omega \right\} + \frac{A_1}{\beta_0} \left\{ \left( \ln(1 - \omega) + \frac{1}{2} \ln(1 - \omega)^2 \right. \right. \right. \\
& \left. \left. \left. + \omega \right) \left( \frac{\beta_1}{\beta_0^2} \right) + \left( \omega \right) L_{fr} + \left( \ln(1 - \omega) \right) L_{qr} \right\} \right], \quad (\text{A.8})
\end{aligned}$$

$$\begin{aligned}
g_3 = & \left[ \frac{A_3}{\beta_0^2} \left\{ -\frac{\omega}{(1 - \omega)} + \omega \right\} + \frac{A_2}{\beta_0} \left\{ \left( 2 \frac{\omega}{(1 - \omega)} \right) L_{qr} + \left( 3 \frac{\omega}{(1 - \omega)} + 2 \frac{\ln(1 - \omega)}{(1 - \omega)} \right. \right. \right. \\
& \left. \left. \left. - \omega \right) \left( \frac{\beta_1}{\beta_0^2} \right) + \left( -2 \omega \right) L_{fr} \right\} + A_1 \left\{ -4 \zeta_2 \frac{\omega}{(1 - \omega)} + \left( -\frac{\ln(1 - \omega)^2}{(1 - \omega)} - \frac{\omega}{(1 - \omega)} \right. \right. \right. \\
& \left. \left. \left. - 2 \frac{\ln(1 - \omega)}{(1 - \omega)} + 2 \ln(1 - \omega) + \omega \right) \left( \frac{\beta_1}{\beta_0^2} \right)^2 + \left( -\frac{\omega}{(1 - \omega)} \right) L_{qr}^2 + \left( -\frac{\omega}{(1 - \omega)} \right) \right\} \right]
\end{aligned}$$

$$\begin{aligned}
& -2 \ln(1-\omega) - \omega \Bigg) \left( \frac{\beta_2}{\beta_0^3} \right) + \left( \left( -2 \frac{\omega}{(1-\omega)} - 2 \frac{\ln(1-\omega)}{(1-\omega)} \right) \left( \frac{\beta_1}{\beta_0^2} \right) \right) L_{qr} \\
& + \left( \omega \right) L_{fr}^2 \Bigg\} + \frac{D_2}{\beta_0} \left\{ \frac{\omega}{(1-\omega)} \right\} + D_1 \left\{ \left( -\frac{\omega}{(1-\omega)} \right) L_{qr} + \left( -\frac{\omega}{(1-\omega)} \right. \right. \\
& \left. \left. - \frac{\ln(1-\omega)}{(1-\omega)} \right) \left( \frac{\beta_1}{\beta_0^2} \right) \right\}, \tag{A.9}
\end{aligned}$$

Here  $A_i$  are the universal cusp anomalous dimensions,  $D_i$  are the threshold non-cusp anomalous dimensions, and  $\omega = 2a_s\beta_0 \ln \bar{N}$ . Note that all the perturbative quantities are expanded in powers of  $a_s$ . The cusp anomalous dimensions  $A_i$  are given as (recently four-loops results are available can be found in Ref. [142–144]),

$$A_1 = C_F \left\{ 4 \right\}, \tag{A.10}$$

$$A_2 = C_F \left\{ n_f \left( -\frac{40}{9} \right) + C_A \left( \frac{268}{9} - 8\zeta_2 \right) \right\}, \tag{A.11}$$

$$\begin{aligned}
A_3 = C_F \left\{ n_f^2 \left( -\frac{16}{27} \right) + C_F n_f \left( -\frac{110}{3} + 32\zeta_3 \right) + C_A n_f \left( -\frac{836}{27} - \frac{112}{3}\zeta_3 + \frac{160}{9}\zeta_2 \right) \right. \\
\left. + C_A^2 \left( \frac{490}{3} + \frac{88}{3}\zeta_3 - \frac{1072}{9}\zeta_2 + \frac{176}{5}\zeta_2^2 \right) \right\}, \tag{A.12}
\end{aligned}$$

The coefficients  $D_i$  are given as,

$$D_1 = C_F \left\{ 0 \right\}, \tag{A.13}$$

$$D_2 = C_F \left\{ n_f \left( \frac{224}{27} - \frac{32}{3}\zeta_2 \right) + C_A \left( -\frac{1616}{27} + 56\zeta_3 + \frac{176}{3}\zeta_2 \right) \right\}, \tag{A.14}$$

Here,

$$C_A = N, \quad C_F = \frac{N^2 - 1}{2N}, \tag{A.15}$$

$$\beta_0 = \frac{11}{3}C_A - \frac{2}{3}n_f, \tag{A.16}$$

$$\beta_1 = \frac{34}{3}C_A^2 - \frac{10}{3}n_f C_A - 2n_f C_F, \tag{A.17}$$

$$\beta_2 = \frac{2857}{54}C_A^3 - \frac{1415}{54}n_f C_A^2 - \frac{205}{18}n_f C_F C_A + n_f C_F^2 + \frac{79}{54}n_f^2 C_A + \frac{11}{9}n_f^2 C_F. \tag{A.18}$$

## References

- [1] CMS collaboration, A. Tumasyan et al., *Measurements of the electroweak diboson production cross sections in proton-proton collisions at  $\sqrt{s} = 5.02$  TeV using leptonic decays*, *Phys. Rev. Lett.* **127** (2021) 191801 [[2107.01137](#)].
- [2] ATLAS collaboration, G. Aad et al., *Measurement of the ZZ production cross section and limits on anomalous neutral triple gauge couplings in proton-proton collisions at  $\sqrt{s} = 7$  TeV with the ATLAS detector*, *Phys. Rev. Lett.* **108** (2012) 041804 [[1110.5016](#)].

- [3] ATLAS collaboration, G. Aad et al., *Measurement of ZZ production in pp collisions at  $\sqrt{s} = 7$  TeV and limits on anomalous ZZZ and ZZ $\gamma$  couplings with the ATLAS detector*, *JHEP* **03** (2013) 128 [[1211.6096](#)].
- [4] CMS collaboration, S. Chatrchyan et al., *Measurement of the ZZ Production Cross Section and Search for Anomalous Couplings in 2 l2l' Final States in pp Collisions at  $\sqrt{s} = 7$  TeV*, *JHEP* **01** (2013) 063 [[1211.4890](#)].
- [5] CMS collaboration, V. Khachatryan et al., *Measurements of the Z Z production cross sections in the 2l2 $\nu$  channel in proton–proton collisions at  $\sqrt{s} = 7$  and 8 TeV and combined constraints on triple gauge couplings*, *Eur. Phys. J. C* **75** (2015) 511 [[1503.05467](#)].
- [6] CMS collaboration, S. Chatrchyan et al., *Measurement of  $W^+W^-$  and ZZ Production Cross Sections in pp Collisions at  $\sqrt{s} = 8$ TeV*, *Phys. Lett. B* **721** (2013) 190 [[1301.4698](#)].
- [7] CMS collaboration, V. Khachatryan et al., *Measurement of the  $pp \rightarrow ZZ$  Production Cross Section and Constraints on Anomalous Triple Gauge Couplings in Four-Lepton Final States at  $\sqrt{s} = 8$  TeV*, *Phys. Lett. B* **740** (2015) 250 [[1406.0113](#)].
- [8] ATLAS collaboration, G. Aad et al., *Measurements of four-lepton production in pp collisions at  $\sqrt{s} = 8$  TeV with the ATLAS detector*, *Phys. Lett. B* **753** (2016) 552 [[1509.07844](#)].
- [9] ATLAS collaboration, M. Aaboud et al., *Measurement of the ZZ production cross section in proton-proton collisions at  $\sqrt{s} = 8$  TeV using the  $ZZ \rightarrow \ell^-\ell^+\ell^-\ell^+$  and  $ZZ \rightarrow \ell^-\ell^+\nu\bar{\nu}$  channels with the ATLAS detector*, *JHEP* **01** (2017) 099 [[1610.07585](#)].
- [10] CMS collaboration, A. M. Sirunyan et al., *Measurement of differential cross sections for Z boson pair production in association with jets at  $\sqrt{s} = 8$  and 13 TeV*, *Phys. Lett. B* **789** (2019) 19 [[1806.11073](#)].
- [11] CMS collaboration, V. Khachatryan et al., *Measurement of the ZZ production cross section and  $Z \rightarrow \ell^+\ell^-\ell^+\ell^-$  branching fraction in pp collisions at  $\sqrt{s}=13$  TeV*, *Phys. Lett. B* **763** (2016) 280 [[1607.08834](#)].
- [12] ATLAS collaboration, M. Aaboud et al.,  *$ZZ \rightarrow \ell^+\ell^-\ell^+\ell^-$  cross-section measurements and search for anomalous triple gauge couplings in 13 TeV pp collisions with the ATLAS detector*, *Phys. Rev. D* **97** (2018) 032005 [[1709.07703](#)].
- [13] CMS collaboration, A. M. Sirunyan et al., *Measurements of the  $pp \rightarrow ZZ$  production cross section and the  $Z \rightarrow 4\ell$  branching fraction, and constraints on anomalous triple gauge couplings at  $\sqrt{s} = 13$  TeV*, *Eur. Phys. J. C* **78** (2018) 165 [[1709.08601](#)].
- [14] ATLAS collaboration, M. Aaboud et al., *Measurement of ZZ production in the  $\ell\ell\nu\nu$  final state with the ATLAS detector in pp collisions at  $\sqrt{s} = 13$  TeV*, *JHEP* **10** (2019) 127 [[1905.07163](#)].
- [15] CMS collaboration, A. M. Sirunyan et al., *Measurements of  $pp \rightarrow ZZ$  production cross sections and constraints on anomalous triple gauge couplings at  $\sqrt{s} = 13$  TeV*, *Eur. Phys. J. C* **81** (2021) 200 [[2009.01186](#)].
- [16] ATLAS collaboration, G. Aad et al., *Measurement of zz production cross-sections in the four-lepton final state in pp collisions at  $s=13.6$ tev with the atlas experiment*, *Physics Letters B* **855** (2024) 138764.
- [17] J. Ohnemus and J. F. Owens, *Order- $\alpha_s$  calculation of hadronic zz production*, *Phys. Rev. D* **43** (1991) 3626.

- [18] B. Mele, P. Nason and G. Ridolfi, *QCD radiative corrections to  $Z$  boson pair production in hadronic collisions*, *Nucl. Phys. B* **357** (1991) 409.
- [19] C. Zecher, T. Matsuura and J. J. van der Bij, *Leptonic signals from off-shell  $Z$  boson pairs at hadron colliders*, *Z. Phys. C* **64** (1994) 219 [[hep-ph/9404295](#)].
- [20] J. Ohnemus, *Hadronic  $ZZ$ ,  $W^-W^+$ , and  $W^\pm Z$  production with QCD corrections and leptonic decays*, *Phys. Rev. D* **50** (1994) 1931 [[hep-ph/9403331](#)].
- [21] J. Ohnemus, *Order  $\alpha^-s$  calculations of hadronic  $W^\pm\gamma$  and  $Z\gamma$  production*, *Phys. Rev. D* **47** (1993) 940.
- [22] U. Baur, T. Han and J. Ohnemus, *QCD corrections to hadronic  $W\gamma$  production with nonstandard  $WW\gamma$  couplings*, *Phys. Rev. D* **48** (1993) 5140 [[hep-ph/9305314](#)].
- [23] U. Baur, T. Han and J. Ohnemus, *QCD corrections and anomalous couplings in  $Z\gamma$  production at hadron colliders*, *Phys. Rev. D* **57** (1998) 2823 [[hep-ph/9710416](#)].
- [24] L. J. Dixon, Z. Kunszt and A. Signer, *Helicity amplitudes for  $O(\alpha_s)$  production of  $W^+W^-$ ,  $W^\pm Z$ ,  $ZZ$ ,  $W^\pm\gamma$ , or  $Z\gamma$  pairs at hadron colliders*, *Nucl. Phys. B* **531** (1998) 3 [[hep-ph/9803250](#)].
- [25] L. J. Dixon, Z. Kunszt and A. Signer, *Vector boson pair production in hadronic collisions at order  $\alpha_s$  : Lepton correlations and anomalous couplings*, *Phys. Rev. D* **60** (1999) 114037 [[hep-ph/9907305](#)].
- [26] J. M. Campbell, R. K. Ellis and C. Williams, *Vector Boson Pair Production at the LHC*, *JHEP* **07** (2011) 018 [[1105.0020](#)].
- [27] T. Melia, P. Nason, R. Rontsch and G. Zanderighi,  *$W+W^-$ ,  $WZ$  and  $ZZ$  production in the POWHEG BOX*, *JHEP* **11** (2011) 078 [[1107.5051](#)].
- [28] P. Nason and G. Zanderighi,  *$W^+W^-$ ,  $WZ$  and  $ZZ$  production in the POWHEG-BOX-V2*, *Eur. Phys. J. C* **74** (2014) 2702 [[1311.1365](#)].
- [29] R. Frederix, S. Frixione, V. Hirschi, F. Maltoni, R. Pittau and P. Torrielli, *Four-lepton production at hadron colliders: aMC@NLO predictions with theoretical uncertainties*, *JHEP* **02** (2012) 099 [[1110.4738](#)].
- [30] N. Agarwal, V. Ravindran, V. K. Tiwari and A. Tripathi,  *$Z$  boson pair production at the LHC to  $O(\alpha_s)$  in TeV scale gravity models*, *Nucl. Phys. B* **830** (2010) 248 [[0909.2651](#)].
- [31] T. Binoth, T. Gleisberg, S. Karg, N. Kauer and G. Sanguinetti, *NLO QCD corrections to  $ZZ$ +jet production at hadron colliders*, *Phys. Lett. B* **683** (2010) 154 [[0911.3181](#)].
- [32] F. Campanario, M. Kerner, L. D. Ninh and D. Zeppenfeld, *Next-to-leading order QCD corrections to  $ZZ$  production in association with two jets*, *JHEP* **07** (2014) 148 [[1405.3972](#)].
- [33] T. Gehrmann, A. von Manteuffel and L. Tancredi, *The two-loop helicity amplitudes for  $q\bar{q}' \rightarrow V_1 V_2 \rightarrow 4$  leptons*, *JHEP* **09** (2015) 128 [[1503.04812](#)].
- [34] F. Cascioli, T. Gehrmann, M. Grazzini, S. Kallweit, P. Maierhöfer, A. von Manteuffel et al.,  *$ZZ$  production at hadron colliders in NNLO QCD*, *Phys. Lett. B* **735** (2014) 311 [[1405.2219](#)].
- [35] G. Heinrich, S. Jahn, S. P. Jones, M. Kerner and J. Pires, *NNLO predictions for  $Z$ -boson pair production at the LHC*, *JHEP* **03** (2018) 142 [[1710.06294](#)].

- [36] M. Grazzini, S. Kallweit and D. Rathlev, *ZZ production at the LHC: fiducial cross sections and distributions in NNLO QCD*, *Phys. Lett. B* **750** (2015) 407 [[1507.06257](#)].
- [37] S. Kallweit and M. Wiesemann, *ZZ production at the LHC: NNLO predictions for  $2\ell 2\nu$  and  $4\ell$  signatures*, *Phys. Lett. B* **786** (2018) 382 [[1806.05941](#)].
- [38] M. Grazzini, S. Kallweit, D. Rathlev and M. Wiesemann,  *$W^\pm Z$  production at the LHC: fiducial cross sections and distributions in NNLO QCD*, *JHEP* **05** (2017) 139 [[1703.09065](#)].
- [39] C. Duhr, F. Dulat and B. Mistlberger, *Drell-Yan Cross Section to Third Order in the Strong Coupling Constant*, *Phys. Rev. Lett.* **125** (2020) 172001 [[2001.07717](#)].
- [40] C. Duhr, F. Dulat and B. Mistlberger, *Charged current Drell-Yan production at  $N^3LO$* , *JHEP* **11** (2020) 143 [[2007.13313](#)].
- [41] C. Duhr and B. Mistlberger, *Lepton-pair production at hadron colliders at  $N^3LO$  in QCD*, *JHEP* **03** (2022) 116 [[2111.10379](#)].
- [42] J. Baglio, C. Duhr, B. Mistlberger and R. Szafron, *Inclusive production cross sections at  $N^3LO$* , *JHEP* **12** (2022) 066 [[2209.06138](#)].
- [43] A. A H, G. Das, M. C. Kumar, P. Mukherjee, V. Ravindran and K. Samanta, *Resummed Drell-Yan cross-section at  $N^3LL$* , *JHEP* **10** (2020) 153 [[2001.11377](#)].
- [44] G. Das, C. Dey, M. C. Kumar and K. Samanta, *Threshold enhanced cross sections for colorless productions*, *Phys. Rev. D* **107** (2023) 034038 [[2210.17534](#)].
- [45] G. Das, C. Dey, M. C. Kumar and K. Samanta, *Precision Studies for Higgs-Strahlung Process at Hadron Collider*, *Springer Proc. Phys.* **304** (2024) 245.
- [46] A. A H, P. Mukherjee and V. Ravindran, *Next to soft corrections to Drell-Yan and Higgs boson productions*, *Phys. Rev. D* **105** (2022) 094035 [[2006.06726](#)].
- [47] A. A H, P. Mukherjee, V. Ravindran, A. Sankar and S. Tiwari, *Next-to SV resummed Drell-Yan cross section beyond leading-logarithm*, *Eur. Phys. J. C* **82** (2022) 234 [[2107.09717](#)].
- [48] A. A H, P. Mukherjee and V. Ravindran, *Going beyond soft plus virtual*, *Phys. Rev. D* **105** (2022) L091503 [[2204.09012](#)].
- [49] P. A. Baikov, K. G. Chetyrkin, A. V. Smirnov, V. A. Smirnov and M. Steinhauser, *Quark and gluon form factors to three loops*, *Phys. Rev. Lett.* **102** (2009) 212002 [[0902.3519](#)].
- [50] T. Gehrmann, E. W. N. Glover, T. Huber, N. Ikizlerli and C. Studerus, *The quark and gluon form factors to three loops in QCD through to  $O(\epsilon^2)$* , *JHEP* **11** (2010) 102 [[1010.4478](#)].
- [51] C. Anastasiou, C. Duhr, F. Dulat and B. Mistlberger, *Soft triple-real radiation for Higgs production at  $N3LO$* , *JHEP* **07** (2013) 003 [[1302.4379](#)].
- [52] C. Anastasiou, C. Duhr, F. Dulat, F. Herzog and B. Mistlberger, *Higgs Boson Gluon-Fusion Production in QCD at Three Loops*, *Phys. Rev. Lett.* **114** (2015) 212001 [[1503.06056](#)].
- [53] F. Dulat, B. Mistlberger and A. Pelloni, *Differential Higgs production at  $N^3LO$  beyond threshold*, *JHEP* **01** (2018) 145 [[1710.03016](#)].
- [54] M. Bonvini and S. Marzani, *Resummed Higgs cross section at  $N^3LL$* , *JHEP* **09** (2014) 007 [[1405.3654](#)].
- [55] M. Bonvini, S. Marzani, C. Muselli and L. Rottoli, *On the Higgs cross section at  $N^3LO+N^3LL$  and its uncertainty*, *JHEP* **08** (2016) 105 [[1603.08000](#)].

[56] T. Ahmed, M. C. Kumar, P. Mathews, N. Rana and V. Ravindran, *Pseudo-scalar Higgs boson production at threshold  $N^3$  LO and  $N^3$  LL QCD*, *Eur. Phys. J. C* **76** (2016) 355 [[1510.02235](#)].

[57] T. Ahmed, M. Bonvini, M. C. Kumar, P. Mathews, N. Rana, V. Ravindran et al., *Pseudo-scalar Higgs boson production at  $N^3$  LO<sub>A</sub> +  $N^3$  LL'*, *Eur. Phys. J. C* **76** (2016) 663 [[1606.00837](#)].

[58] A. A H, P. Mukherjee, V. Ravindran, A. Sankar and S. Tiwari, *Resummed Higgs boson cross section at next-to SV to NNLO +  $\overline{\text{NNLL}}$* , *Eur. Phys. J. C* **82** (2022) 774 [[2109.12657](#)].

[59] A. Bhattacharya, M. C. Kumar, P. Mathews and V. Ravindran, *Next-to-soft-virtual resummed prediction for pseudoscalar Higgs boson production at NNLO+NNLL<sup>-</sup>*, *Phys. Rev. D* **105** (2022) 116015 [[2112.02341](#)].

[60] A. A H, A. Chakraborty, G. Das, P. Mukherjee and V. Ravindran, *Resummed prediction for Higgs boson production through  $b\bar{b}$  annihilation at  $N^3$  LL*, *JHEP* **11** (2019) 006 [[1905.03771](#)].

[61] G. Das and A. Sankar, *Next-to-soft threshold effects on Higgs boson production via bottom quark annihilation*, [2409.01553](#).

[62] P. Banerjee, G. Das, P. K. Dhani and V. Ravindran, *Threshold resummation of the rapidity distribution for Drell-Yan production at NNLO+NNLL*, *Phys. Rev. D* **98** (2018) 054018 [[1805.01186](#)].

[63] G. Das,  *$Z, W^\pm$  rapidity distributions at NNLL and beyond*, [2303.16578](#).

[64] A. A H, P. Mukherjee, V. Ravindran, A. Sankar and S. Tiwari, *Next-to-soft corrections for Drell-Yan and Higgs boson rapidity distributions beyond  $N^3$  LO*, *Phys. Rev. D* **103** (2021) L111502 [[2010.00079](#)].

[65] T. Ahmed, A. A H, P. Mukherjee, V. Ravindran and A. Sankar, *Rapidity distribution at soft-virtual and beyond for  $n$ -colorless particles to  $N^4$  LO in QCD*, *Eur. Phys. J. C* **81** (2021) 943 [[2010.02980](#)].

[66] A. A H, P. Mukherjee, V. Ravindran, A. Sankar and S. Tiwari, *Next-to-soft-virtual resummed rapidity distribution for the Drell-Yan process to NNLO+NNLL<sup>-</sup>*, *Phys. Rev. D* **106** (2022) 034005 [[2112.14094](#)].

[67] V. Ravindran, A. Sankar and S. Tiwari, *Rapidity distribution of pseudoscalar Higgs boson to NNLOA+NNLL<sup>-</sup>*, *Phys. Rev. D* **110** (2024) 016019 [[2309.14833](#)].

[68] T. Ahmed, M. K. Mandal, N. Rana and V. Ravindran, *Rapidity Distributions in Drell-Yan and Higgs Productions at Threshold to Third Order in QCD*, *Phys. Rev. Lett.* **113** (2014) 212003 [[1404.6504](#)].

[69] T. Ahmed, M. Mahakhud, N. Rana and V. Ravindran, *Drell-Yan Production at Threshold to Third Order in QCD*, *Phys. Rev. Lett.* **113** (2014) 112002 [[1404.0366](#)].

[70] M. C. Kumar, M. K. Mandal and V. Ravindran, *Associated production of Higgs boson with vector boson at threshold  $N^3$  LO in QCD*, *JHEP* **03** (2015) 037 [[1412.3357](#)].

[71] M. Bonvini, S. Marzani, J. Rojo, L. Rottoli, M. Ubiali, R. D. Ball et al., *Parton distributions with threshold resummation*, *JHEP* **09** (2015) 191 [[1507.01006](#)].

[72] L. Rottoli and M. Bonvini, *Towards small- $x$  resummed parton distribution functions*, *PoS DIS2017* (2018) 207 [[1707.01535](#)].

[73] P. Banerjee, G. Das, P. K. Dhani and V. Ravindran, *Threshold resummation of the rapidity distribution for Higgs production at NNLO+NNLL*, *Phys. Rev. D* **97** (2018) 054024 [[1708.05706](#)].

[74] V. Ravindran, A. Sankar and S. Tiwari, *Resummed next-to-soft corrections to rapidity distribution of Higgs boson to NNLO+NNLL<sup>-</sup>*, *Phys. Rev. D* **108** (2023) 014012 [[2205.11560](#)].

[75] G. Das, *Higgs boson rapidity distribution in bottom annihilation at NNLL and beyond*, *Phys. Rev. D* **108** (2023) 094028 [[2306.04561](#)].

[76] M. Grazzini, S. Kallweit, D. Rathlev and M. Wiesemann, *Transverse-momentum resummation for vector-boson pair production at NNLL+NNLO*, *JHEP* **08** (2015) 154 [[1507.02565](#)].

[77] J. M. Campbell, R. K. Ellis, T. Neumann and S. Seth, *Transverse momentum resummation at  $N^3LL+NNLO$  for diboson processes*, *JHEP* **03** (2023) 080 [[2210.10724](#)].

[78] L. Buonocore, G. Koole, D. Lombardi, L. Rottoli, M. Wiesemann and G. Zanderighi, *ZZ production at  $nNNLO+PS$  with MiNNLO<sub>PS</sub>*, *JHEP* **01** (2022) 072 [[2108.05337](#)].

[79] T. Binoth, N. Kauer and P. Mertsch, *Gluon-induced QCD corrections to  $pp \rightarrow ZZ \rightarrow l\bar{l} l\bar{l}$  anti- $l$  anti- $l$ -prime anti- $l$ -prime*, in *16th International Workshop on Deep Inelastic Scattering and Related Subjects*, p. 142, 7, 2008, [0807.0024](#), DOI.

[80] F. Caola, K. Melnikov, R. Röntsch and L. Tancredi, *QCD corrections to ZZ production in gluon fusion at the LHC*, *Phys. Rev. D* **92** (2015) 094028 [[1509.06734](#)].

[81] M. Grazzini, S. Kallweit, M. Wiesemann and J. Y. Yook, *ZZ production at the LHC: NLO QCD corrections to the loop-induced gluon fusion channel*, *JHEP* **03** (2019) 070 [[1811.09593](#)].

[82] M. Grazzini, S. Kallweit, M. Wiesemann and J. Y. Yook, *Four lepton production in gluon fusion: Off-shell Higgs effects in NLO QCD*, *Phys. Lett. B* **819** (2021) 136465 [[2102.08344](#)].

[83] B. Agarwal, S. Jones, M. Kerner and A. von Manteuffel, *Complete NLO QCD Corrections to ZZ Production in Gluon Fusion*, [2404.05684](#).

[84] S. Alioli, F. Caola, G. Luisoni and R. Röntsch, *ZZ production in gluon fusion at NLO matched to parton-shower*, *Phys. Rev. D* **95** (2017) 034042 [[1609.09719](#)].

[85] A. Bierweiler, T. Kasprzik and J. H. Kühn, *Vector-boson pair production at the LHC to  $\mathcal{O}(\alpha^3)$  accuracy*, *JHEP* **12** (2013) 071 [[1305.5402](#)].

[86] M. Grazzini, S. Kallweit, J. M. Lindert, S. Pozzorini and M. Wiesemann, *NNLO QCD + NLO EW with Matrix+OpenLoops: precise predictions for vector-boson pair production*, *JHEP* **02** (2020) 087 [[1912.00068](#)].

[87] A. Denner and G. Pelliccioli, *NLO EW and QCD corrections to polarized ZZ production in the four-charged-lepton channel at the LHC*, *JHEP* **10** (2021) 097 [[2107.06579](#)].

[88] Y. Wang, C. S. Li, Z. L. Liu and D. Y. Shao, *Threshold resummation for  $W^\pm Z$  and ZZ pair production at the LHC*, *Phys. Rev. D* **90** (2014) 034008 [[1406.1417](#)].

[89] CMS collaboration, A. M. Sirunyan et al., *Measurement of the differential Drell-Yan cross section in proton-proton collisions at  $\sqrt{s} = 13$  TeV*, *JHEP* **12** (2019) 059 [[1812.10529](#)].

[90] ATLAS collaboration, G. Aad et al., *Measurement of the high-mass Drell-Yan differential*

*cross-section in  $pp$  collisions at  $\sqrt{s}=7$  TeV with the ATLAS detector, *Phys. Lett. B* **725** (2013) 223 [[1305.4192](#)].*

[91] FCC collaboration, A. Abada et al., *FCC-hh: The Hadron Collider: Future Circular Collider Conceptual Design Report Volume 3*, *Eur. Phys. J. ST* **228** (2019) 755.

[92] S. A. Larin, *Theoretical aspects of quantum field theory*, *Journal of Theoretical Physics* **27** (1993) 123.

[93] S. Moch, J. A. M. Vermaseren and A. Vogt, *Three-loop results for quark and gluon form-factors*, *Phys. Lett. B* **625** (2005) 245 [[hep-ph/0508055](#)].

[94] S. Moch, J. A. M. Vermaseren and A. Vogt, *The Quark form-factor at higher orders*, *JHEP* **08** (2005) 049 [[hep-ph/0507039](#)].

[95] T. Gehrmann, E. W. N. Glover, T. Huber, N. Ikizlerli and C. Studerus, *Calculation of the quark and gluon form factors to three loops in QCD*, *JHEP* **06** (2010) 094 [[1004.3653](#)].

[96] T. Gehrmann and D. Kara, *The  $Hb\bar{b}$  form factor to three loops in QCD*, *JHEP* **09** (2014) 174 [[1407.8114](#)].

[97] S. Moch, J. A. M. Vermaseren and A. Vogt, *The Three loop splitting functions in QCD: The Nonsinglet case*, *Nucl. Phys. B* **688** (2004) 101 [[hep-ph/0403192](#)].

[98] A. Vogt, S. Moch and J. A. M. Vermaseren, *The Three-loop splitting functions in QCD: The Singlet case*, *Nucl. Phys. B* **691** (2004) 129 [[hep-ph/0404111](#)].

[99] J. Blümlein, P. Marquard, C. Schneider and K. Schönwald, *The three-loop unpolarized and polarized non-singlet anomalous dimensions from off shell operator matrix elements*, *Nucl. Phys. B* **971** (2021) 115542 [[2107.06267](#)].

[100] V. V. Sudakov, *Vertex parts at very high-energies in quantum electrodynamics*, *Sov. Phys. JETP* **3** (1956) 65.

[101] A. H. Mueller, *On the Asymptotic Behavior of the Sudakov Form-factor*, *Phys. Rev. D* **20** (1979) 2037.

[102] J. C. Collins, *Algorithm to Compute Corrections to the Sudakov Form-factor*, *Phys. Rev. D* **22** (1980) 1478.

[103] A. Sen, *Asymptotic Behavior of the Sudakov Form-Factor in QCD*, *Phys. Rev. D* **24** (1981) 3281.

[104] G. F. Sterman, *Summation of Large Corrections to Short Distance Hadronic Cross-Sections*, *Nucl. Phys. B* **281** (1987) 310.

[105] S. Catani and L. Trentadue, *Resummation of the QCD Perturbative Series for Hard Processes*, *Nucl. Phys. B* **327** (1989) 323.

[106] S. Catani and L. Trentadue, *Comment on QCD exponentiation at large  $x$* , *Nucl. Phys. B* **353** (1991) 183.

[107] N. Kidonakis and G. F. Sterman, *Resummation for QCD hard scattering*, *Nucl. Phys. B* **505** (1997) 321 [[hep-ph/9705234](#)].

[108] N. Kidonakis, *A Unified approach to NNLO soft and virtual corrections in electroweak, Higgs, QCD, and SUSY processes*, *Int. J. Mod. Phys. A* **19** (2004) 1793 [[hep-ph/0303186](#)].

[109] V. Ravindran, *On Sudakov and soft resummations in QCD*, *Nucl. Phys. B* **746** (2006) 58 [[hep-ph/0512249](#)].

[110] V. Ravindran, *Higher-order threshold effects to inclusive processes in QCD*, *Nucl. Phys. B* **752** (2006) 173 [[hep-ph/0603041](#)].

[111] S. Moch, J. A. M. Vermaasen and A. Vogt, *Higher-order corrections in threshold resummation*, *Nucl. Phys. B* **726** (2005) 317 [[hep-ph/0506288](#)].

[112] E. Laenen and L. Magnea, *Threshold resummation for electroweak annihilation from DIS data*, *Phys. Lett. B* **632** (2006) 270 [[hep-ph/0508284](#)].

[113] N. Kidonakis, *Next-to-next-to-next-to-leading-order soft-gluon corrections in hard-scattering processes near threshold*, *Phys. Rev. D* **73** (2006) 034001 [[hep-ph/0509079](#)].

[114] A. Idilbi, X.-d. Ji and F. Yuan, *Resummation of threshold logarithms in effective field theory for DIS, Drell-Yan and Higgs production*, *Nucl. Phys. B* **753** (2006) 42 [[hep-ph/0605068](#)].

[115] S. Catani, D. de Florian, M. Grazzini and P. Nason, *Soft gluon resummation for Higgs boson production at hadron colliders*, *JHEP* **07** (2003) 028 [[hep-ph/0306211](#)].

[116] A. A H and H.-S. Shao,  *$N^3LO+N^3LL$  QCD improved Higgs pair cross sections*, *JHEP* **02** (2023) 067 [[2209.03914](#)].

[117] T. O. Eynck, E. Laenen and L. Magnea, *Exponentiation of the Drell-Yan cross-section near partonic threshold in the DIS and MS-bar schemes*, *JHEP* **06** (2003) 057 [[hep-ph/0305179](#)].

[118] G. Das, S.-O. Moch and A. Vogt, *Soft corrections to inclusive deep-inelastic scattering at four loops and beyond*, *JHEP* **03** (2020) 116 [[1912.12920](#)].

[119] A. H. Ajjath, G. Das, M. C. Kumar, P. Mukherjee, V. Ravindran and K. Samanta, *Resummed Drell-Yan cross-section at  $N^3LL$* , *JHEP* **10** (2020) 153 [[2001.11377](#)].

[120] T. Ahmed, A. H. Ajjath, G. Das, P. Mukherjee, V. Ravindran and S. Tiwari, *Soft-virtual correction and threshold resummation for  $n$ -colorless particles to fourth order in QCD: Part I*, [2010.02979](#).

[121] B. Ruijl, T. Ueda and J. A. M. Vermaasen, *FORM version 4.2*, [1707.06453](#).

[122] A. Vogt, *Efficient evolution of unpolarized and polarized parton distributions with QCD-PEGASUS*, *Comput. Phys. Commun.* **170** (2005) 65 [[hep-ph/0408244](#)].

[123] S. Catani, M. L. Mangano, P. Nason and L. Trentadue, *The Resummation of soft gluons in hadronic collisions*, *Nucl. Phys. B* **478** (1996) 273 [[hep-ph/9604351](#)].

[124] E. L. Berger and H. Contopanagos, *Threshold resummation of the total cross-section for heavy quark production in hadronic collisions*, *Phys. Rev. D* **57** (1998) 253 [[hep-ph/9706206](#)].

[125] N. Kidonakis, *High order corrections and subleading logarithms for top quark production*, *Phys. Rev. D* **64** (2001) 014009 [[hep-ph/0010002](#)].

[126] S. Forte, G. Ridolfi, J. Rojo and M. Ubiali, *Borel resummation of soft gluon radiation and higher twists*, *Phys. Lett. B* **635** (2006) 313 [[hep-ph/0601048](#)].

[127] N. Kidonakis, *Soft-gluon corrections in top-quark production*, *Int. J. Mod. Phys. A* **33** (2018) 1830021 [[1806.03336](#)].

[128] P. Hinderer, F. Ringer, G. Sterman and W. Vogelsang, *Threshold Resummation at NNLL for Single-particle Production in Hadronic Collisions*, *Phys. Rev. D* **99** (2019) 054019 [[1812.00915](#)].

[129] S. Catani, *The singular behaviour of qcd amplitudes at two-loop order*, *Physics Letters B* **427** (1998) 161–171.

[130] L. Naterop, A. Signer and Y. Ulrich, *handyG —Rapid numerical evaluation of generalised polylogarithms in Fortran*, *Comput. Phys. Commun.* **253** (2020) 107165 [[1909.01656](#)].

[131] M. Grazzini, S. Kallweit and M. Wiesemann, *Fully differential NNLO computations with MATRIX*, *Eur. Phys. J. C* **78** (2018) 537 [[1711.06631](#)].

[132] A. Denner, S. Dittmaier and L. Hofer, *Collier: a fortran-based Complex One-Loop Library in Extended Regularizations*, *Comput. Phys. Commun.* **212** (2017) 220 [[1604.06792](#)].

[133] F. Caccioli, P. Maierhofer and S. Pozzorini, *Scattering Amplitudes with Open Loops*, *Phys. Rev. Lett.* **108** (2012) 111601 [[1111.5206](#)].

[134] F. Buccioni, J.-N. Lang, J. M. Lindert, P. Maierh”ofer, S. Pozzorini, H. Zhang et al., *OpenLoops 2*, *Eur. Phys. J. C* **79** (2019) 866 [[1907.13071](#)].

[135] F. Buccioni, S. Pozzorini and M. Zoller, *On-the-fly reduction of open loops*, *Eur. Phys. J. C* **78** (2018) 70 [[1710.11452](#)].

[136] G. Das, M. C. Kumar and K. Samanta, *Precision QCD phenomenology of exotic spin-2 search at the LHC*, *JHEP* **04** (2021) 111 [[2011.15121](#)].

[137] S. Bailey, T. Cridge, L. A. Harland-Lang, A. D. Martin and R. S. Thorne, *Parton distributions from LHC, HERA, Tevatron and fixed target data: MSHT20 PDFs*, *Eur. Phys. J. C* **81** (2021) 341 [[2012.04684](#)].

[138] A. Buckley, J. Ferrando, S. Lloyd, K. Nordström, B. Page, M. Rüfenacht et al., *LHAPDF6: parton density access in the LHC precision era*, *Eur. Phys. J. C* **75** (2015) 132 [[1412.7420](#)].

[139] J. Alwall, M. Herquet, F. Maltoni, O. Mattelaer and T. Stelzer, *Madgraph 5: going beyond*, *Journal of High Energy Physics* **2011** (2011) .

[140] G. Das, M. C. Kumar and K. Samanta, *Resummed inclusive cross-section in ADD model at  $N^3LL$* , *JHEP* **10** (2020) 161 [[1912.13039](#)].

[141] G. Das, M. C. Kumar and K. Samanta, *Resummed inclusive cross-section in Randall-Sundrum model at NNLO+NNLL*, *JHEP* **07** (2020) 040 [[2004.03938](#)].

[142] J. M. Henn, M. Stahlhofen, M. Steinhauser and M. Wormser, *Matter dependence of the four-loop QCD cusp anomalous dimension: from small angles to all angles*, *JHEP* **04** (2020) 003 [[1911.10174](#)].

[143] T. Huber, T. Hurth, E. Lunghi and J. Virto, *Logarithmically Enhanced Contributions to the Angular Observables in  $B \rightarrow V\ell\ell$* , *JHEP* **08** (2019) 152 [[1905.00965](#)].

[144] A. von Manteuffel, R. M. Schabinger and H. X. Zhu, *The two-loop soft function for heavy quark pair production at future linear colliders*, *JHEP* **08** (2020) 068 [[2003.01798](#)].